

©2019 Optical Society of America. Access to this work was provided by the University of Maryland, Baltimore County (UMBC) ScholarWorks@UMBC digital repository on the Maryland Shared Open Access (MD-SOAR) platform.

Please provide feedback

Please support the ScholarWorks@UMBC repository by emailing scholarworks-group@umbc.edu and telling us what having access to this work means to you and why it's important to you. Thank you.



Turbulence-free two-photon double-slit interference with coherent and incoherent light

THOMAS A. SMITH*  AND YANHUA SHIH

Department of Physics, University of Maryland, Baltimore County, Baltimore, MD 21250, USA

*tsmith25@umbc.edu

Abstract: This article reports a study on a turbulence-free Young's double-slit interferometer. When the environmental turbulence blurs out the classic Young's double-slit interference completely, a two-photon interference pattern is still observable from the measurement of intensity or photon number fluctuation correlation. This two-photon interferometer always produces a turbulence-free interference pattern, when the double-slit interferometer is utilizing both first-order spatially incoherent light and spatially coherent light. This type of two-photon interferometer establishes new capabilities in optical observations and sensing measurements that require high sensitivity and stability.

© 2019 Optical Society of America under the terms of the [OSA Open Access Publishing Agreement](#)

1. Introduction

Interferometers utilize the property of superposition of radiation fields to make accurate measurements and have many uses in a wide range of fields [1–6]. A classic, or first-order, interferometer measures the intensity of light, or the photon flux of radiation, which, by means of optical delays between the superposed electromagnetic fields (or the superposed amplitudes of a photon), gives rise to an interference pattern in the output current of a photodetector. Likewise, a two-photon interferometer, or second-order interferometer, measures the intensity fluctuation correlation or photon number fluctuation correlation which gives rise to an interference pattern in the joint-photodetection of two photodetectors by means of manipulating the optical delay between the superposed two-photon amplitudes of a pair of photons. Often two-photon interference is associated with light in an entangled state [7–9]; however, as originally done in the Hanbury Brown-Twiss experiment [10,11], two-photon interference with randomly created and randomly distributed thermal light is also been demonstrated [12,13]. Many interferometers can be negatively affected by the fluctuations resulting from optical turbulence in the environment, especially over large distances [14,15]. This forces extremely sensitive interferometers to be contained in high-cost vacuum chambers, such as the ones required for the Laser Interferometer Gravitational-Wave Observatory (LIGO) [16]. Is optical turbulence always harmful to interferometers? It has been demonstrated recently in a Young's double-slit interferometer that optical turbulence is not necessarily harmful to two-photon double-slit interference under certain conditions [17]. The demonstrations of two-photon double-slit interference [12] and turbulence-free double-slit interference [17] exclusively utilized the experimental condition of $d \gg l_c$, where d is the separation of the two slits and l_c is the spatial coherence of the applied light, such that no first-order interference was observable.

This article reports a general study of the two-photon double-slit interferometer including when $d \ll l_c$ in which the classic first-order interference from the measurement of intensity or photon flux is observable. We show that spatially incoherent light is not a requirement for two-photon interference with 100% visibility. When $d \ll l_c$, both first-order and second-order interference are observable; however, when the environmental turbulence blurs out the classic Young's double-slit interference completely, a two-photon interference pattern is still present. How does a two-photon interferometer overcome turbulence and produce interference when the classic Young's double-slit interference pattern is blurred? And why is the turbulence-free nature

of two-photon interference independent of first-order spatial coherence? This article addresses these fundamentally interesting and practically useful questions.

This article is organized as follows: in Sec. II we review the concept of intensity fluctuations due to interference between two photons based on Einstein's granularity picture of thermal light and distinguish these fluctuations from the classical changes in mean intensity. Also reviewed is the concept of the intensity fluctuation correlation, which is the measurement of two-photon interference: a randomly created and randomly pair of subfields, or photons, interfering with the pair itself. A brief subsection is included to demonstrate the equivalence of Glauber's theory of optical coherence to Einstein's picture of thermal light and place emphasis on the concept of two-photon interference. Applying this model of two-photon interference in Sec. III we compare the measurements of intensity fluctuation correlation and intensity following a double slit. Specifically, we focus on how different degrees of first order spatial coherence affect both types of measurements. Following this, we then analyze what effect optical turbulence has on both measurements and provide experimental data in Sec. IV. Section V then summarizes our conclusions.

2. Intensity fluctuations and two-photon interference

The reported two-photon double-slit interferometer consists of light from a disk-like thermal source incident on a double slit, similar to the classic Young's double-slit interferometer [1,18]; however, now two detectors, D_1 and D_2 , jointly measure the intensity fluctuation correlation, $\langle \Delta I(\mathbf{r}_1, t_1) \Delta I(\mathbf{r}_2, t_2) \rangle$, or equivalently in photon counting mode, the photon number fluctuation correlation $\langle \Delta n(\mathbf{r}_1, t_1) \Delta n(\mathbf{r}_2, t_2) \rangle$. For the measurements discussed in this paper we will focus on the second-order spatial correlation by assuming perfect second-order temporal correlation through the use of monochromatic thermal light. To simplify the mathematics, we also only focus on the 1-D spatial measurement in the form of $\langle \Delta I(x_1) \Delta I(x_2) \rangle$ or $\langle \Delta n(x_1) \Delta n(x_2) \rangle$. The interference present in this measurement is a result of two-photon interference: two randomly created and randomly paired photons interfering with the pair itself [19,20].

2.1. Einstein's granularity picture

To model these measurements we will use Einstein's granularity picture of thermal light [21]. This picture models the total electric field from electromagnetic radiation at detector D_j as a superposition of a large number of quantized subfields (corresponding to photons in modern language),

$$E(\mathbf{r}_j, t_j) = \sum_m E_m(\mathbf{r}_j, t_j) = \sum_m E_m g_m(\mathbf{r}_j, t_j), \quad (1)$$

where $E_m = a_m e^{i\phi_m}$ labels the complex amplitude of a subfield emitted from the m th subsurface with a random phase ϕ_m , and $g_m(\mathbf{r}_j, t_j)$ represents the field propagator or Green's function that propagates the m th subfield from the coordinate of the subsurface (\mathbf{r}_m, t_m) to the coordinate of the detector (\mathbf{r}_j, t_j) . The intensity, or the first-order correlation, measured by detector D_j at (\mathbf{r}_j, t_j) is $\langle I(\mathbf{r}_j, t_j) \rangle = \langle E^*(\mathbf{r}_j, t_j) E(\mathbf{r}_j, t_j) \rangle$, which can be written as

$$\begin{aligned} \langle I(\mathbf{r}_j, t_j) \rangle &= \left\langle \sum_m E_m^*(\mathbf{r}_j, t_j) \sum_n E_n(\mathbf{r}_j, t_j) \right\rangle \\ &= \left\langle \sum_m |E_m(\mathbf{r}_j, t_j)|^2 \right\rangle + \left\langle \sum_{m \neq n} E_m^*(\mathbf{r}_j, t_j) E_n(\mathbf{r}_j, t_j) \right\rangle \\ &= \sum_m |E_m(\mathbf{r}_j, t_j)|^2 + 0. \end{aligned} \quad (2)$$

The expectation value, or ensemble average, takes into account all possible phases and, due to the random phase difference between the m th and n th subfields, the $m \neq n$ term sums

to zero. In a typical measurement, not all random phases may be present, meaning the $m \neq n$ term will contribute to the measurement. We may conclude that the mean intensity, $\langle I(\mathbf{r}_j, t_j) \rangle = \sum_m |E_m(\mathbf{r}_j, t_j)|^2$, is the result of the m th subfield interfering with the m th subfield itself and that the m th subfield interfering with a different n th subfield results in fluctuations in intensity, $\Delta I(\mathbf{r}_j, t_j) = \sum_{m \neq n} E_m^*(\mathbf{r}_j, t_j) E_n(\mathbf{r}_j, t_j)$. Although these fluctuations are typically considered as unwanted noise, the correlation of intensity fluctuations at separate detectors may not be considered as noise,

$$\begin{aligned} \langle \Delta I(\mathbf{r}_1, t_1) \Delta I(\mathbf{r}_2, t_2) \rangle &= \left\langle \sum_{m \neq n} E_m^*(\mathbf{r}_1, t_1) E_n(\mathbf{r}_1, t_1) \sum_{p \neq q} E_p^*(\mathbf{r}_2, t_2) E_q(\mathbf{r}_2, t_2) \right\rangle \\ &= \sum_{m \neq n} E_m^*(\mathbf{r}_1, t_1) E_n(\mathbf{r}_1, t_1) E_n^*(\mathbf{r}_2, t_2) E_m(\mathbf{r}_2, t_2). \end{aligned} \quad (3)$$

Due to the cancellation of random relative phases between the subfields, the $m = q$ and $n = p$ terms survive the ensemble average. Mathematically, the result of Eq. (3) is the cross term of the following superposition,

$$\sum_{m \neq n} |E_m(\mathbf{r}_1, t_1) E_n(\mathbf{r}_2, t_2) + E_n(\mathbf{r}_1, t_1) E_m(\mathbf{r}_2, t_2)|^2, \quad (4)$$

corresponding to the superposition of two different yet indistinguishable alternatives of joint photodetection: (1) the m th subfield is measured at D_1 while the n th subfield is measured at D_2 ; (2) the n th subfield is measured at D_1 while the m th subfield is measured at D_2 . Physically, the above superposition defines two-photon interference: a random pair of subfields (photons) interfering with the pair itself. In its entirety, Eq. (4) is equivalent to the intensity-intensity correlation of thermal light,

$$\begin{aligned} \langle I(\mathbf{r}_1, t_1) I(\mathbf{r}_2, t_2) \rangle &= \sum_{m \neq n} \frac{1}{\sqrt{2}} [E_m(\mathbf{r}_1, t_1) E_n(\mathbf{r}_2, t_2) + E_n(\mathbf{r}_1, t_1) E_m(\mathbf{r}_2, t_2)]^2 \\ &= \sum_m |E_m(\mathbf{r}_1, t_1)|^2 \sum_n |E_n(\mathbf{r}_2, t_2)|^2 + \sum_{m \neq n} E_m^*(\mathbf{r}_1, t_1) E_n(\mathbf{r}_1, t_1) E_n^*(\mathbf{r}_2, t_2) E_m(\mathbf{r}_2, t_2) \\ &= \langle I(\mathbf{r}_1, t_1) \rangle \langle I(\mathbf{r}_2, t_2) \rangle + \langle \Delta I(\mathbf{r}_1, t_1) \Delta I(\mathbf{r}_2, t_2) \rangle. \end{aligned} \quad (5)$$

Note that, in this notation, $\langle \Delta I(\mathbf{r}_1, t_1) \Delta I(\mathbf{r}_2, t_2) \rangle$ refers to the two-photon interference induced intensity fluctuation correlation. In addition to the fluctuations from the m th subfield interfering with the n th subfield, $\langle I(\mathbf{r}_1, t_1) \rangle = \sum_m |E_m(\mathbf{r}_1, t_1)|^2$ and $\langle I(\mathbf{r}_2, t_2) \rangle = \sum_n |E_n(\mathbf{r}_2, t_2)|^2$ may fluctuate from time to time or from measurement to measurement due to the variation of the total number of subfields (photons) that contribute to each measurement. These changes in total photons present in the system may be better labeled as “classical” intensity fluctuations while the two-photon interference induced fluctuations resulting from $\sum_{m \neq n} E_m^*(\mathbf{r}_j, t_j) E_n(\mathbf{r}_j, t_j)$ may be considered quantum fluctuations or quantum noise.

2.2. Glauber's theory of optical coherence

To fully connect Einstein's granularity picture of thermal light to the idea of two-photon interference we can look toward the quantum theory of optical coherence [19,22,23]. Following Glauber's theory, we introduce a concept of the “effective wavefunction.” It can be shown that the effective wavefunction of a photon in the thermal state takes the same mathematical form as that of Einstein's quantized subfield. One can write the state of thermal field in coherent state representation: $|\Psi\rangle = \prod_m |\alpha_m\rangle$, where m labels the m th photon or the m th group of identical photons that are in the coherent state $|\alpha_m\rangle$. The field operator at (\mathbf{r}_j, t_j) , for $j = 1, 2$ indicating the

j th photodetector, can be written as,

$$\begin{aligned}\hat{E}^{(+)}(\mathbf{r}_j, t_j) &= \sum_m \int d\mathbf{k} \hat{a}_m(\mathbf{k}) g_m(\mathbf{k}; \mathbf{r}_j, t_j) \\ \hat{E}^{(-)}(\mathbf{r}_j, t_j) &= \sum_m \int d\mathbf{k} \hat{a}_m^\dagger(\mathbf{k}) g_m^*(\mathbf{k}; \mathbf{r}_j, t_j)\end{aligned}\quad (6)$$

where $g_m(\mathbf{k}; \mathbf{r}_j, t_j)$ is the same Green's function (or propagator) used in Einstein's picture which propagates the \mathbf{k} mode of the state from the space-time coordinate of emission, (\mathbf{r}_m, t_m) , to D_j at space-time coordinate (\mathbf{r}_j, t_j) . The first-order coherence function is calculated as follows,

$$\begin{aligned}G^{(1)}(\mathbf{r}_1, t_1) &= \langle \langle \Psi | \hat{E}^{(-)}(\mathbf{r}_1, t_1) \hat{E}^{(+)}(\mathbf{r}_1, t_1) | \Psi \rangle \rangle_{Es} \\ &= \langle \langle \Psi | \sum_m \hat{E}_m^{(-)}(\mathbf{r}_1, t_1) \sum_n \hat{E}_n^{(+)}(\mathbf{r}_1, t_1) | \Psi \rangle \rangle_{Es} \\ &= \left\langle \sum_{m=n} |\psi_m(\mathbf{r}_1, t_1)|^2 \right\rangle_{Es} + \left\langle \sum_{m \neq n} \psi_m^*(\mathbf{r}_1, t_1) \psi_n(\mathbf{r}_1, t_1) \right\rangle_{Es} \\ &= \langle n(\mathbf{r}_1, t_1) \rangle + 0,\end{aligned}\quad (7)$$

for which we have defined the effective wavefunction of the m th photon (or coherent group of photons) as,

$$\psi_m(\mathbf{r}_1, t_1) = \int d\mathbf{k} \alpha_m(\mathbf{k}) g_m(\mathbf{k}; \mathbf{r}_1, t_1). \quad (8)$$

It is clear that this effective wavefunction has the same mathematical form as Einstein's quantized subfield presented in Eq. (1) and the first-order coherence function in Eq. (7) is the same as that in Einstein's picture, except Einstein's quantized subfield is replaced by the effective wavefunction.

A similar equivalence is found with the second-order coherence function,

$$\begin{aligned}G^{(2)}(\mathbf{r}_1, t_1; \mathbf{r}_2, t_2) &= \langle \langle \Psi | \sum_m \hat{E}_m^{(-)}(\mathbf{r}_1, t_1) \sum_n \hat{E}_n^{(-)}(\mathbf{r}_2, t_2) \sum_p \hat{E}_p^{(+)}(\mathbf{r}_2, t_2) \sum_q \hat{E}_q^{(+)}(\mathbf{r}_1, t_1) | \Psi \rangle \rangle_{Es} \\ &= \left\langle \sum_m |\psi_m(\mathbf{r}_1, t_1)|^2 \right\rangle_{Es} \left\langle \sum_n |\psi_n(\mathbf{r}_2, t_2)|^2 \right\rangle_{Es} + \left\langle \sum_{m \neq n} \psi_m^*(\mathbf{r}_1, t_1) \psi_n(\mathbf{r}_1, t_1) \psi_n^*(\mathbf{r}_2, t_2) \psi_m(\mathbf{r}_2, t_2) \right\rangle_{Es} \\ &= \sum_{m,n} |\psi_m(\mathbf{r}_1, t_1) \psi_n(\mathbf{r}_2, t_2) + \psi_n(\mathbf{r}_1, t_1) \psi_m(\mathbf{r}_2, t_2)|^2 \\ &= \langle n(\mathbf{r}_1, t_1) \rangle \langle n(\mathbf{r}_2, t_2) \rangle + \langle \Delta n(\mathbf{r}_1, t_1) \Delta n(\mathbf{r}_2, t_2) \rangle.\end{aligned}\quad (9)$$

We find that this result matches that of Eq. (5) and that the measurement is a result of interference involving a superposition between quantum amplitudes $A_1 = \psi_m(\mathbf{r}_1, t_1) \psi_n(\mathbf{r}_2, t_2)$ and $A_2 = \psi_n(\mathbf{r}_1, t_1) \psi_m(\mathbf{r}_2, t_2)$ corresponding to two possible ways to achieve a joint photo-detection event: (1) the m th photon is measured at D_1 while the n th photon is measured at D_2 ; (2) the n th photon is measured at D_1 while the m th photon is measured at D_2 . This equivalence emphasizes that the measurement of intensity fluctuation correlation or photon number fluctuation correlation is a result of a random pair of photons interfering with the pair itself, namely two-photon interference.

3. Double-slit interferometer

The Green's function varies dependent on the potential optical paths. For free propagation without turbulence, such as the propagation of a subfield from the subsource to a specific slit (or

from the slit to a detector), $g_m(\mathbf{r}_j, t_j)$ is of the form,

$$g_m(\mathbf{r}_j, t_j) = \int d\mathbf{k} g_m(\mathbf{k}; \mathbf{r}_j, t_j) \simeq \int d\mathbf{k} e^{i[\mathbf{k} \cdot (\mathbf{r}_j - \mathbf{r}_m) - \omega(t_j - t_m)]}, \quad (10)$$

where $g_m(\mathbf{k}; \mathbf{r}_j, t_j)$ is the Green's function for propagating each mode of \mathbf{k} . When measuring a 1-D spatial scan in Fresnel near-field, this can be approximated as,

$$g_m(x_j) = e^{ikz} e^{i\frac{k}{2z}(x_j - x_m)^2} = e^{i\frac{2\pi n_0 z}{\lambda}} e^{i\frac{\pi n_0}{\lambda z}(x_j - x_m)^2} \quad (11)$$

where we have assumed a monochromatic field to simplify the calculation. Propagating the m th subfield from the m th subsource to slit-A and slit-B, respectively, and then to D_j at x_j can be represented by the following superposition,

$$g_m(x_j) = \frac{1}{\sqrt{2}} [g_{mA}(x_j) + g_{mB}(x_j)], \quad (12)$$

where $g_{mA}(x_j) = g_m(x_A)g_A(x_j)$ and $g_{mB}(x_j) = g_m(x_B)g_B(x_j)$.

3.1. Spatially coherent double-slit measurements

For the specific case of a point-like thermal light source emitting monochromatic light onto slit-A and slit-B symmetrically with equal optical paths, the fields at slit-A and slit-B are considered spatially and temporally first-order coherent. Due to the first-order coherence of the fields passing through slit-A and slit-B, we find both terms of Eq. (5) yield a product of classic Young's double-slit interference

$$\begin{aligned} \langle I(x_1) \rangle \langle I(x_2) \rangle &= I_0^2 \cos^2 \frac{\pi n_0 d}{\lambda z} x_1 \cos^2 \frac{\pi n_0 d}{\lambda z} x_2 \\ \langle \Delta I(x_1) \Delta I(x_2) \rangle &= I_0^2 \cos^2 \frac{\pi n_0 d}{\lambda z} x_1 \cos^2 \frac{\pi n_0 d}{\lambda z} x_2, \end{aligned} \quad (13)$$

where n_0 is the index of refraction of the light propagating medium, d is the separation between slit-A and slit-B, λ is the wavelength of the light in a vacuum, and z is the distance from the slits to the detectors. To simplify the mathematics we have assumed narrow, line-like slits. Classic Young's double-slit interference is observable in the measurement of intensity at each photodetector (and thus the product of the two measurements), as well as in the measurement of two-photon interference induced intensity fluctuation correlation $\langle \Delta I(x_1) \Delta I(x_2) \rangle$. In the measurement of $\langle I(x_1) I(x_2) \rangle$ we thus have

$$\langle I(x_1) I(x_2) \rangle = 2I_0^2 \cos^2 \frac{\pi n_0 d}{\lambda z} x_1 \cos^2 \frac{\pi n_0 d}{\lambda z} x_2. \quad (14)$$

3.2. Spatially incoherent double-slit measurements

Next, we consider a disk-like thermal source with angular diameter $\Delta\theta_s \approx D_s/z_s$, where D_s is the source diameter and z_s is the distance from the source to the slits as depicted in Fig. 1. We can once again propagate the field from the source to the detector D_j with the Green's function of Eq. (12), but now we account for the size of the source by approximating the summation of subfields as an integral from $-\Delta\theta_s/2$ to $\Delta\theta_s/2$. The measurement of intensity at a single detector

is calculated as follows,

$$\begin{aligned}\langle I(x_j) \rangle &= \frac{1}{2} \sum_m |E_m|^2 |g_{mA}(x_j) + g_{mB}(x_j)|^2 \\ &= \frac{I_0}{2\Delta\theta_s} \int_{-\Delta\theta_s/2}^{\Delta\theta_s/2} d\theta_m |g_{mA}(x_j) + g_{mB}(x_j)|^2 \\ &= \frac{I_0}{2} \left[1 + \text{sinc} \frac{\pi n_0 d \Delta\theta_s}{\lambda} \cos \frac{2\pi n_0 d}{\lambda z} x_j \right],\end{aligned}\quad (15)$$

where the sinc function is defined as $\text{sinc}(x) = \sin(x)/x$. It is easy to see that when $d > \lambda/n_0\Delta\theta_s$, the sinc function vanishes and there is no observable interference. The spatial coherence length is often defined as $l_c \equiv \lambda/n_0\Delta\theta_s$. We can calculate the visibility of this first-order interference pattern as,

$$V \equiv \frac{I_{max} - I_{min}}{I_{max} + I_{min}} = \text{sinc} \frac{\pi n_0 d \Delta\theta_s}{\lambda}. \quad (16)$$

The fields at slit-A and slit-B are considered spatially incoherent when $d > l_c$ and the output of the sinc function is approximately zero, resulting in zero visibility. Contrarily, the fields at slit-A and slit-B are considered spatially coherent as $l_c \rightarrow \infty$ causing the sinc function to take a value of one and the visibility of the interference pattern to become 100%. When the sinc function takes a value between zero and one, the fields at slit-A and slit-B are considered partially spatially coherent. Partially coherent fields would still produce a first-order interference pattern in each measurement of $\langle I(x_j) \rangle$, although with reduced visibility, and thus produce a product of first-order interference patterns in $\langle I(x_1) \rangle \langle I(x_2) \rangle$,

$$\langle I(x_1) \rangle \langle I(x_2) \rangle = \frac{I_0^2}{4} \left[1 + \text{sinc} \frac{\pi n_0 d \Delta\theta_s}{\lambda} \cos \frac{2\pi n_0 d}{\lambda z} x_1 \right] \left[1 + \text{sinc} \frac{\pi n_0 d \Delta\theta_s}{\lambda} \cos \frac{2\pi n_0 d}{\lambda z} x_2 \right]. \quad (17)$$

If one were to scan the two detectors in unison such that $x_1 = x_2$, the resulting visibility would be,

$$V = \frac{2\text{sinc}[\pi n_0 d \Delta\theta_s / \lambda]}{1 + \text{sinc}^2[\pi n_0 d \Delta\theta_s / \lambda]}. \quad (18)$$

Additionally, if one were to scan one detector while the other is held stationary, the visibility would be the same as first-order interference,

$$V = \text{sinc} \frac{\pi n_0 d \Delta\theta_s}{\lambda}. \quad (19)$$

The intensity fluctuation correlation, however, provides a different interference pattern when the fields at slit-A and slit-B are partially coherent. For this measurement, we can apply Eq. (12) to Eq. (3) and obtain the following,

$$\begin{aligned}\langle \Delta I(x_1) \Delta I(x_2) \rangle &= \frac{1}{4} \sum_{m \neq n} |E_m|^2 |E_n|^2 [g_{mA}(x_1) + g_{mB}(x_1)]^* [g_{nA}(x_1) + g_{nB}(x_1)] \\ &\quad \times [g_{nA}(x_2) + g_{nB}(x_2)]^* [g_{mA}(x_2) + g_{mB}(x_2)].\end{aligned}\quad (20)$$

This results in 16 terms which can be represented by

$$\langle \Delta I(x_1) \Delta I(x_2) \rangle = \sum_{ijkl} \langle \Delta I(x_1)_{ij} \Delta I(x_2)_{kl} \rangle, \quad (21)$$

where

$$\langle \Delta I(x_1)_{ij} \Delta I(x_2)_{kl} \rangle = \frac{1}{4} \sum_{m \neq n} |E_m|^2 |E_n|^2 g_{mi}^*(x_1) g_{nj}(x_1) g_{nk}^*(x_2) g_{ml}(x_2), \quad (22)$$

for $i, j, k, l = A, B$. These terms are expanded upon in Appendix A. Combining the results into a compact form we get,

$$\langle \Delta I(x_1) \Delta I(x_2) \rangle = I_0^2 \left[\cos \frac{\pi n_0 d}{\lambda z} (x_1 - x_2) + \text{sinc} \frac{\pi n_0 d \Delta \theta_s}{\lambda} \cos \frac{\pi n_0 d}{\lambda z} (x_1 + x_2) \right]^2, \quad (23)$$

where, once again, the angular diameter of the source affects the outcome of the measurement. In the limiting case of spatially coherent fields, $l_c \rightarrow \infty$, the sinc function can be approximated as one, leading to x_1 becoming separable from x_2 , resulting in Eq. (13). Note that under these conditions, if either detector is held stationary at a location where the intensity is at a minimum, i.e. $\langle I(x_j) \rangle = 0$, then no interference will be present in the measurement of $\langle \Delta I(x_1) \Delta I(x_2) \rangle$ while scanning the second detector.

In the case of partially coherent fields, as in Eq. (23), there are multiple scanning arrangements that achieve 100% visibility. Examples include: (1) when D_1 and D_2 are scanned simultaneously maintaining $x_1 + x_2 = m\lambda z / 2n_0 d$, where m is an integer, such that only one cosine term remains in Eq. (23); (2) when D_1 and D_2 are scanned simultaneously maintaining $x_1 - x_2 = m\lambda z / 2n_0 d$, likewise allowing only one cosine term to be present; or (3) when either detector is held stationary, such as at $x_2 = 0$, while the second is scanned. Interestingly, when scanning the detectors in unison such that $x_1 = x_2$, the measurement of intensity fluctuation correlation is proportional to the result of Eq. (17) when $x_1 = x_2$ and thus has the same visibility given in Eq. (18).

This 100% visibility is also easily obtained when the fields passing through each slit are fully spatially incoherent, $d \gg l_c$, for which, unlike first-order interference which gets blurred completely, certain two-photon interference terms remain resulting in,

$$\langle \Delta I(x_1) \Delta I(x_2) \rangle = I_0^2 \cos^2 \frac{\pi n_0 d}{\lambda z} (x_1 - x_2). \quad (24)$$

First demonstrated by Scarcelli *et al.* [12], here the positions of D_1 and D_2 are non-separable, exhibiting the non-classical effects of this measurement.

3.3. The effect of optical turbulence

Another condition that may reduce the visibility of the double-slit interference pattern is when optical turbulence is present between the slits and detector(s). Optical turbulence is defined as a random change in index of refraction, δn_{ij} , dependent on the optical path from each slit $i = A, B$ to detector $j = 1, 2$ (for this discussion, we will ignore potential scattering). These changes are related to the mean index of refraction, n_0 , such that $n_{ij} = n_0 + \delta n_{ij}$. In general, if a medium of volume V has a random spatial distribution of index of refraction that also varies in time, $n(\mathbf{r}, t)$, then the mean index of refraction of that volume over the total time of measurement τ is,

$$n_0 = \frac{1}{V} \int_V d\mathbf{r} \frac{1}{\tau} \int_{\tau} dt n(\mathbf{r}, t). \quad (25)$$

Similarly, the mean index of refraction along a potential path of propagation at a specific moment for a single photon is,

$$n_{ij} = \frac{1}{|\mathbf{r}_j - \mathbf{r}_i|} \int_{\mathbf{r}_i}^{\mathbf{r}_j} d\mathbf{r} \frac{1}{|t_j - t_i|} \int_{t_i}^{t_j} dt n(\mathbf{r}, t). \quad (26)$$

It should be noted that for our analysis, $n(\mathbf{r}, t)$ can take any form; however, for more extreme cases, scattering may become more prevalent, which we have not accounted for.

Accounting for turbulence we will use a Green's function with the same form as Eq. (11) but with the random shift in index of refraction included,

$$g_i^T(x_j) = e^{i\frac{2\pi n_{ij}z}{\lambda}} e^{i\frac{\pi n_{ij}}{\lambda z}(x_j-x_i)^2} = e^{i\frac{2\pi n_0 z}{\lambda}} e^{i\frac{\pi n_0}{\lambda z}(x_j-x_i)^2} e^{i\frac{2\pi \delta n_{ij} z}{\lambda}} e^{i\frac{\pi \delta n_{ij}}{\lambda z}(x_j-x_i)^2} \quad (27)$$

Here it is useful to define a random phase shift of $\delta\phi_{ij} = \frac{2\pi \delta n_{ij}}{\lambda}(z + (x_j - x_i)^2/2z)$ such that,

$$g_i^T(x_j) = e^{i\frac{2\pi n_0 z}{\lambda}} e^{i\frac{\pi n_0}{\lambda z}(x_j-x_i)^2} e^{i\delta\phi_{ij}} = g_i(x_j) e^{i\delta\phi_{ij}}, \quad (28)$$

where now this random phase shift, which is dependent on the change in index of refraction from the mean, is applied to the original Green's function given in Eq. (11).

When calculating the expectation value of intensity, an integral over all possible phases present is needed in addition to the integral over the angular diameter of the source. This was not needed originally because the relative phases were the same. We have defined $\phi_j = \delta\phi_{ij} - \delta\phi_{ij}$ for $i = A, B$ as the phase difference between the potential paths of a single subfield detected at D_j and integrating over all possible phase differences results in,

$$\begin{aligned} \langle I(x_j) \rangle &= \frac{I_0}{2\Delta\theta_s} \int_{-\Delta\theta_s/2}^{\Delta\theta_s/2} d\theta_m \frac{1}{\Delta\phi} \int_{-\Delta\phi/2}^{\Delta\phi/2} d\phi_j |g_{mA}^T(x_j) + g_{mB}^T(x_j)|^2 \\ &= \frac{I_0}{2} \left[1 + \text{sinc}\Delta\phi \text{sinc}\frac{\pi n_0 d \Delta\theta_s}{\lambda} \cos\frac{2\pi n_0 d}{\lambda z} x_j \right], \end{aligned} \quad (29)$$

where $\Delta\phi$ is the *range* of possible phase differences. Here we have approximated a uniform distribution of possible phase difference over a certain range. If there is no turbulence present, there is never a difference in phase introduced between paths from slits A and B so $\Delta\phi = 0$, leaving the original interference pattern achieved in Eq. (15). If the turbulence is strong enough such that range of possible random phase shift differences is large, i.e. $\Delta\phi \gg \pi$, only the constant term will remain, resulting in no interference.

To predict the effect of turbulence on two-photon double-slit interference, we will continue to model the optical turbulence as done in Eq. (28). Applying it to Eq. (22) we get,

$$\langle \Delta I(x_1)_{ij} \Delta I(x_2)_{kl} \rangle = \frac{1}{4} \sum_{m \neq n} |E_m|^2 |E_n|^2 g_{mi}^*(x_1) e^{-i\delta\phi_{i1}} g_{nj}(x_1) e^{i\delta\phi_{j1}} g_{nk}^*(x_2) e^{-i\delta\phi_{k2}} g_{ml}(x_2) e^{i\delta\phi_{l2}}, \quad (30)$$

for $i, j, k, l = A, B$. Recall that this measurement is a result of two-photon interference and can be written as the cross terms of the superposition of a pair of two-photon probability amplitudes, similar to Eq. (4),

$$\langle I(x_1)_{ij} I(x_2)_{kl} \rangle = \sum_{m \neq n} |E_{mi}(x_1) e^{i\delta\phi_{i1}} E_{nk}(x_2) e^{i\delta\phi_{k2}} + E_{nj}(x_1) e^{i\delta\phi_{j1}} E_{ml}(x_2) e^{i\delta\phi_{l2}}|^2. \quad (31)$$

It is easy to see in Eq. (30) that when both $i = j$ and $k = l$, these random phase shifts cancel. It should be noted that this is independent of the distribution of turbulence, $n(\mathbf{r}, t)$, and specifically occurs because the paths through the turbulence are the same. This results in $\langle \Delta I(x_1)_{AA} \Delta I(x_2)_{AA} \rangle$, $\langle \Delta I(x_1)_{BB} \Delta I(x_2)_{BB} \rangle$, $\langle \Delta I(x_1)_{AA} \Delta I(x_2)_{BB} \rangle$, and $\langle \Delta I(x_1)_{BB} \Delta I(x_2)_{AA} \rangle$ all being insensitive to turbulence, i.e. turbulence free. In addition to these, more terms have the potential to be turbulence free, specifically when both $i = l$ and $j = k$ and when the two detectors, D_1 and D_2 , are in approximately the same location, $x_1 \approx x_2$. This proximity is relative to the spatial distribution of the turbulence such that the two-photon amplitudes (potential paths) overlap and experience the same turbulence (Fig. 1). The new terms that become turbulence free under this condition are $\langle \Delta I(x_1)_{AB} \Delta I(x_2)_{BA} \rangle$ and $\langle \Delta I(x_1)_{BA} \Delta I(x_2)_{AB} \rangle$. In total, the six terms that

remain present through turbulence with partially spatially coherent light result in the following interference pattern,

$$\langle \Delta I(x_1) \Delta I(x_2) \rangle = I_0^2 \left[\frac{1}{2} \text{sinc}^2 \frac{\pi n_0 d \Delta \theta_s}{\lambda} + \cos^2 \frac{\pi n_0 d}{\lambda z} (x_1 - x_2) \right]. \quad (32)$$

This result is elaborated upon in Appendix B. Comparing this to the general case without turbulence, Eq. (23), which had multiple ways of obtaining 100% visibility, now this is only achievable with a spatially incoherent source of $d \gg l_c$ (as done in the turbulence-free double-slit interferometer). However, with a partially or fully spatially coherent source, a new constant term is present which lowers the visibility of the interference pattern. In general, the visibility of this measurement is,

$$V = \frac{1}{1 + \text{sinc}^2[\pi n_0 d \Delta \theta_s / \lambda]}. \quad (33)$$

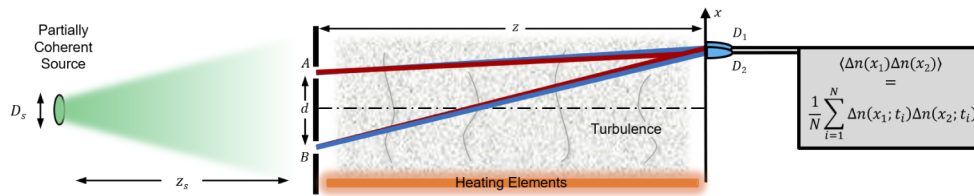


Fig. 1. Overlap of two-photon amplitudes. In the figure, the superposed two different yet indistinguishable two-photon amplitudes are indicated by red and blue colors. When the detectors are scanning in the neighborhood of $x_1 \approx x_2$, the red amplitude and the blue amplitude “overlap” which means the pair experience the same phase variations, resulting in an interference pattern insensitive to turbulence.

4. Experiment

The initial demonstration of the turbulence-free double-slit interferometer utilized spatially incoherent light in order to produce a turbulence-free interference pattern that maintained 100% visibility. The experiment presented in this article utilizes partially spatially coherent light to demonstrate how interference still remains visible through optical turbulence (Fig. 2). In lieu of a true thermal source, which typically have more bandwidth, a standard monochromatic pseudo-thermal light source is used consisting of a rotating ground glass and a single-frequency laser beam of wavelength $\lambda = 532$ nm [24]. Millions of tiny diffusers within the rotating ground glass scatter the laser beam into many independent wave packets, or subfields, at the single-photon level with random relative phases, artificially simulating a natural thermal light. An adjustable pinhole is used to control the transverse size of the light source, allowing us to alter the spatial coherence length of the thermal field. By placing a double-slit with line-like slits and a slit separation of $d = 2.5$ mm, 7.5 m after the pinhole, we achieved an angular diameter of $\Delta \theta_s \approx 0.000124$ and thus obtained a spatial coherence length of $l_c = \lambda / n_0 \Delta \theta_s \approx 4.3$ mm. Point-like tips of single-mode fiber collect the light and direct it to single-photon counting detectors (Perkin-Elmer SPCM-AQR). A Photon Number Fluctuation Correlation (PNFC) circuit [25] is then used to measure the mean photon number for each detector, $\langle n(x_1) \rangle$ and $\langle n(x_2) \rangle$, while simultaneously calculating the photon number fluctuation correlation, $\langle \Delta n(x_1) \Delta n(x_2) \rangle$.

To introduce turbulence stronger than what is typically present in the atmosphere, heating elements were used. Temperature variations in the air induce spatial and temporal fluctuations in index of refraction. Figure 3 reports the measurement of photon number fluctuation correlation with and without turbulence present. Each plot compares the predicted theory of Eq. (23)

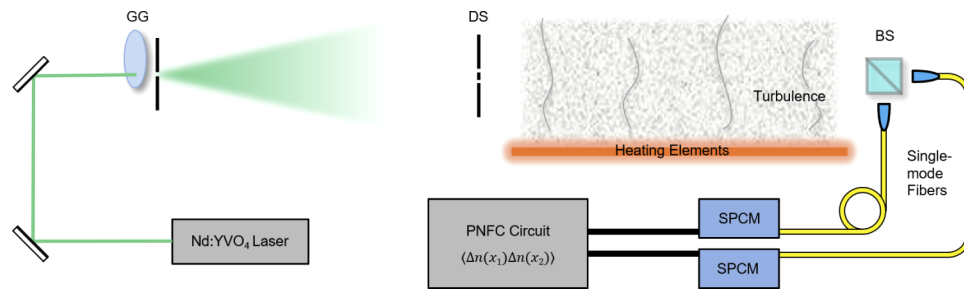


Fig. 2. Experimental setup. Similar to the turbulence-free double-slit interferometer, a pseudo-thermal light source is directed at a pair of slits, except now the source is far enough away to be partially coherent, $l_c > d$. Beyond the slits, point-like tips of single mode fibers collect light and direct it to a pair of single-photon detectors (Perkin-Elmer SPCM-AQR). A Photon Number Fluctuation Correlation (PNFC) circuit then measures the photon number fluctuation correlation $\langle \Delta n(x_1) \Delta n(x_2) \rangle$.

and Eq. (32) in blue with the experimental results in black. For these measurements, D_2 was stationary at $x_2 = 0$ while D_1 was scanned along the x -axis. The experimental results without turbulence, Fig. 3(a), have a visibility of 87.4% which closely matches the predicted 100%. When turbulence is introduced, Fig. 3(b), the 78.7% visibility of the experimental results almost exactly matches the 78.2% visibility predicted by the theory. Both sets of data have been normalized such that $I_0 = 1$ so that the relative amplitudes of the interference patterns can be compared. As expected, the amplitude of the interference pattern with turbulence is lower due to only six of the original sixteen terms being unaffected by the turbulence. We also see that, unlike the turbulence-free double-slit interferometer which uses a spatially incoherent source [17], 100% visibility is *not* maintained with turbulence present when using a partially coherent source; however, the interference pattern is still clearly present.

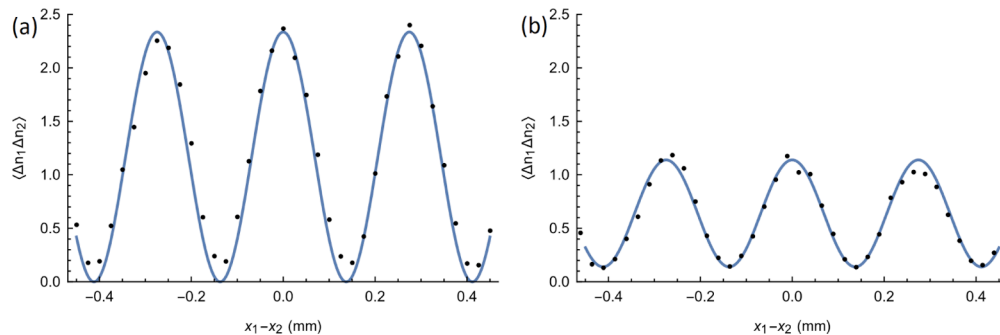


Fig. 3. Typical measurement of $\langle \Delta n(x_1) \Delta n(x_2) \rangle$ when scanning x_1 and x_2 is stationary. (a) Without turbulence present, the interference pattern has a large amplitude and approximately 100% visibility. (b) With turbulence present, certain terms no longer contribute to the measurement, thus lowering the amplitude and decreasing the visibility.

For comparison, Fig. 4 presents the measurement of intensity (mean photon number) obtained from the same measurements used in the intensity fluctuation correlation Fig. 3. Initially without turbulence, as seen in Fig. 4(a), the interference pattern is clearly present, however with reduced visibility due to the source being only partially spatially coherent. As seen in Fig. 4(b), when turbulence is introduced, the interference pattern is blurred completely. Even

with turbulence strong enough to completely blur the interference from the measurement of $\langle n(x_1) \rangle$, the interference from the measurement of $\langle \Delta n(x_1) \Delta n(x_2) \rangle$ is still present.

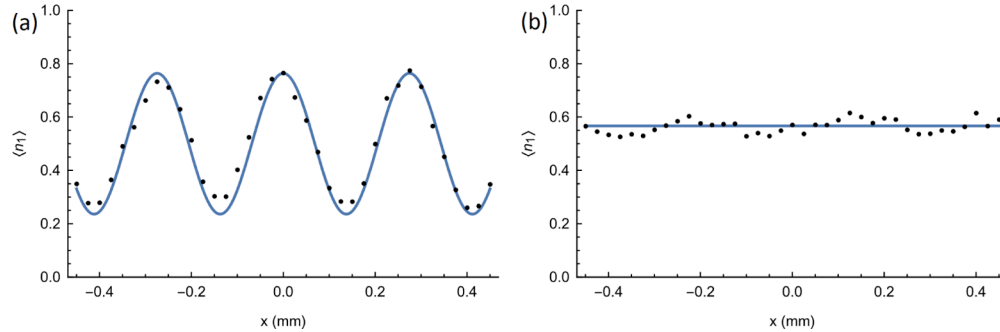


Fig. 4. Typical measurement of $\langle n(x_1) \rangle$ when scanning x_1 . (a) As expected with a partially coherent source, the interference pattern does not have 100% visibility, but an interference pattern is still clearly visible. (b) After introducing turbulence, the interference pattern is blurred completely.

5. Summary

It is interesting to find that the intensity fluctuations of thermal light resulting from two randomly created and randomly paired photons, or subfields, interfering with each other are not necessarily harmful to all interferometers. Instead, the measurement of intensity fluctuation correlation utilizes these intensity fluctuations through two-photon interference in a way that benefits interferometers and interferometric sensors in their sensitivity and stability. This model of two-photon interference is able to accurately predict how the superpositions of different two-photon amplitudes contribute to an interference pattern under different degrees of spatial coherence. This two-photon double-slit interference is observable with 100% visibility in the measurement of intensity fluctuation correlation for both spatially coherent and spatially incoherent light. In addition to this, when scanning one detector D_1 in approximately the same location as D_2 , $x_1 \approx x_2$, interference remains visible through optical turbulence. Unlike when spatially incoherent light is used, which maintains 100% visibility through turbulence, we found that use of spatially coherent light loses some visibility. However, a full interference pattern remains present and is predictable with the two-photon interference theory. The results of the reported experiment are helpful in furthering the fundamental understanding of two-photon interferometry and turbulence-free interferometry.

Appendix A

The result of measuring two-photon double-slit interference through intensity fluctuation correlation as shown in Eq. (20). The resulting 16 terms can be written as,

$$\langle \Delta I(x_1) \Delta I(x_2) \rangle = \sum_{ijkl} \langle \Delta I(x_1)_{ij} \Delta I(x_2)_{kl} \rangle, \tag{34}$$

where

$$\langle \Delta I(x_1)_{ij} \Delta I(x_2)_{kl} \rangle = \frac{1}{4} \sum_{m \neq n} |E_m|^2 |E_n|^2 g_{mi}^*(x_1) g_{nj}(x_1) g_{nk}^*(x_2) g_{ml}(x_2), \tag{35}$$

for $i, j, k, l = A, B$. These terms can be split into groups that provide similar results. When all four potential paths of subfields pass through the same slit, a constant is produced,

$$\begin{aligned} \langle \Delta I(x_1)_{AA} \Delta I(x_2)_{AA} \rangle + \langle \Delta I(x_1)_{BB} \Delta I(x_2)_{BB} \rangle &= \frac{I_0}{2\Delta\theta_s} \int_{-\Delta\theta_s/2}^{\Delta\theta_s/2} d\theta_m \frac{I_0}{2\Delta\theta_s} \int_{-\Delta\theta_s/2}^{\Delta\theta_s/2} d\theta_n \\ &\times [g_{mA}^*(x_1)g_{nA}(x_1)g_{nA}^*(x_2)g_{mA}(x_2) + g_{mB}^*(x_1)g_{nB}(x_1)g_{nB}^*(x_2)g_{mB}(x_2)] \\ &= \frac{1}{2}I_0^2. \end{aligned} \quad (36)$$

Similarly, when a pair of potential paths pass through each slit and then each respective pair travels to the same detector, a constant term that is dependent on the angular diameter of the source is produced,

$$\begin{aligned} \langle \Delta I(x_1)_{AA} \Delta I(x_2)_{BB} \rangle + \langle \Delta I(x_1)_{BB} \Delta I(x_2)_{AA} \rangle &= \frac{I_0}{2\Delta\theta_s} \int_{-\Delta\theta_s/2}^{\Delta\theta_s/2} d\theta_m \frac{I_0}{2\Delta\theta_s} \int_{-\Delta\theta_s/2}^{\Delta\theta_s/2} d\theta_n \\ &\times [g_{mA}^*(x_1)g_{nA}(x_1)g_{nB}^*(x_2)g_{mB}(x_2) + g_{mB}^*(x_1)g_{nB}(x_1)g_{nA}^*(x_2)g_{mA}(x_2)] \\ &= \frac{1}{2}I_0^2 \text{sinc}^2 \frac{\pi d \Delta\theta_s}{\lambda}. \end{aligned} \quad (37)$$

The following four terms all result in a contribution directly comparable to the result of measuring intensity with no dependence on x_2 ,

$$\begin{aligned} \langle \Delta I(x_1)_{AB} \Delta I(x_2)_{AA} \rangle + \langle \Delta I(x_1)_{BA} \Delta I(x_2)_{BB} \rangle + \langle \Delta I(x_1)_{AB} \Delta I(x_2)_{BB} \rangle + \langle \Delta I(x_1)_{BA} \Delta I(x_2)_{AA} \rangle &= \\ \frac{I_0}{2\Delta\theta_s} \int_{-\Delta\theta_s/2}^{\Delta\theta_s/2} d\theta_m \frac{I_0}{2\Delta\theta_s} \int_{-\Delta\theta_s/2}^{\Delta\theta_s/2} d\theta_n & \\ \times [g_{mA}^*(x_1)g_{nB}(x_1)g_{nA}^*(x_2)g_{mA}(x_2) + g_{mB}^*(x_1)g_{nA}(x_1)g_{nB}^*(x_2)g_{mB}(x_2) & \\ + g_{mA}^*(x_1)g_{nB}(x_1)g_{nB}^*(x_2)g_{mB}(x_2) + g_{mB}^*(x_1)g_{nA}(x_1)g_{nA}^*(x_2)g_{mA}(x_2)] & \\ = I_0^2 \text{sinc} \frac{\pi d \Delta\theta_s}{\lambda} \cos \frac{2\pi d}{\lambda z} x_1. & \end{aligned} \quad (38)$$

Likewise, four terms contribute a similar result, but with no dependence on x_1 ,

$$\begin{aligned} \langle \Delta I(x_1)_{AA} \Delta I(x_2)_{AB} \rangle + \langle \Delta I(x_1)_{BB} \Delta I(x_2)_{BA} \rangle + \langle \Delta I(x_1)_{AA} \Delta I(x_2)_{BA} \rangle + \langle \Delta I(x_1)_{BB} \Delta I(x_2)_{AB} \rangle &= \\ \frac{I_0}{2\Delta\theta_s} \int_{-\Delta\theta_s/2}^{\Delta\theta_s/2} d\theta_m \frac{I_0}{2\Delta\theta_s} \int_{-\Delta\theta_s/2}^{\Delta\theta_s/2} d\theta_n & \\ \times [g_{mA}^*(x_1)g_{nA}(x_1)g_{nA}^*(x_2)g_{mB}(x_2) + g_{mB}^*(x_1)g_{nB}(x_1)g_{nB}^*(x_2)g_{mA}(x_2) & \\ + g_{mA}^*(x_1)g_{nA}(x_1)g_{nB}^*(x_2)g_{mA}(x_2) + g_{mB}^*(x_1)g_{nB}(x_1)g_{nA}^*(x_2)g_{mB}(x_2)] & \\ = I_0^2 \text{sinc} \frac{\pi d \Delta\theta_s}{\lambda} \cos \frac{2\pi d}{\lambda z} x_2. & \end{aligned} \quad (39)$$

The next pair of terms result in an interference term that is dependent on both x_1 and x_2 while having no dependence on the angular diameter of the source,

$$\begin{aligned} \langle \Delta I(x_1)_{AB} \Delta I(x_2)_{BA} \rangle + \langle \Delta I(x_1)_{BA} \Delta I(x_2)_{AB} \rangle &= \frac{I_0}{2\Delta\theta_s} \int_{-\Delta\theta_s/2}^{\Delta\theta_s/2} d\theta_m \frac{I_0}{2\Delta\theta_s} \int_{-\Delta\theta_s/2}^{\Delta\theta_s/2} d\theta_n \\ &\times [g_{mA}^*(x_1)g_{nB}(x_1)g_{nB}^*(x_2)g_{mA}(x_2) + g_{mB}^*(x_1)g_{nA}(x_1)g_{nA}^*(x_2)g_{mB}(x_2)] \\ &= \frac{1}{2}I_0^2 \cos \frac{2\pi d}{\lambda z} (x_1 - x_2). \end{aligned} \quad (40)$$

Comparably, this pair results in an interference term that is dependent on both x_1 and x_2 , however this one does have dependence on the angular diameter of the source,

$$\begin{aligned} \langle \Delta I(x_1)_{AB} \Delta I(x_2)_{AB} \rangle + \langle \Delta I(x_1)_{BA} \Delta I(x_2)_{BA} \rangle &= \frac{I_0}{2\Delta\theta_s} \int_{-\Delta\theta_s/2}^{\Delta\theta_s/2} d\theta_m \frac{I_0}{2\Delta\theta_s} \int_{-\Delta\theta_s/2}^{\Delta\theta_s/2} d\theta_n \\ &\times [g_{mA}^*(x_1)g_{nB}(x_1)g_{nA}^*(x_2)g_{mB}(x_2) + g_{mB}^*(x_1)g_{nA}(x_1)g_{nB}^*(x_2)g_{mA}(x_2)] \\ &= \frac{1}{2} I_0^2 \text{sinc}^2 \frac{\pi d \Delta\theta_s}{\lambda} \cos \frac{2\pi d}{\lambda z} (x_1 + x_2). \end{aligned} \quad (41)$$

Combining all of these we get,

$$\begin{aligned} \langle \Delta I(x_1) \Delta I(x_2) \rangle &= \frac{1}{2} I_0^2 \left[1 + \text{sinc}^2 \frac{\pi d \Delta\theta_s}{\lambda} + 2 \text{sinc} \frac{\pi d \Delta\theta_s}{\lambda} \cos \frac{2\pi d}{\lambda z} x_1 + 2 \text{sinc} \frac{\pi d \Delta\theta_s}{\lambda} \cos \frac{2\pi d}{\lambda z} x_2 \right. \\ &\quad \left. + \cos \frac{2\pi d}{\lambda z} (x_1 - x_2) + \text{sinc}^2 \frac{\pi d \Delta\theta_s}{\lambda} \cos \frac{2\pi d}{\lambda z} (x_1 + x_2) \right], \end{aligned} \quad (42)$$

which can be manipulated to be written as Eq. (23).

Appendix B

With turbulence present, the resulting 16 terms can still be written as,

$$\langle \Delta I(x_1) \Delta I(x_2) \rangle = \sum_{ijkl} \langle \Delta I(x_1)_{ij} \Delta I(x_2)_{kl} \rangle, \quad (43)$$

where now a random phase shift is included to each path,

$$\langle \Delta I(x_1)_{ij} \Delta I(x_2)_{kl} \rangle = \frac{1}{4} \sum_{m \neq n} |E_m|^2 |E_n|^2 g_{mi}^*(x_1) e^{-i\delta\phi_{i1}} g_{nj}(x_1) e^{i\delta\phi_{j1}} g_{nk}^*(x_2) e^{-i\delta\phi_{k2}} g_{ml}(x_2) e^{i\delta\phi_{l2}}, \quad (44)$$

for $i, j, k, l = A, B$. As done in Appendix A, these terms can be split into groups that provide similar results. The first pair of constant terms are inherently overlapped and thus the random phase shifts always cancel,

$$\begin{aligned} &\langle \Delta I(x_1)_{AA} \Delta I(x_2)_{AA} \rangle + \langle \Delta I(x_1)_{BB} \Delta I(x_2)_{BB} \rangle \\ &= \frac{I_0}{2\Delta\theta_s} \int_{-\Delta\theta_s/2}^{\Delta\theta_s/2} d\theta_m \frac{I_0}{2\Delta\theta_s} \int_{-\Delta\theta_s/2}^{\Delta\theta_s/2} d\theta_n \frac{1}{\Delta\phi} \int_{-\Delta\phi/2}^{\Delta\phi/2} d\phi_1 \frac{1}{\Delta\phi} \int_{-\Delta\phi/2}^{\Delta\phi/2} d\phi_2 \\ &\times [g_{mA}^*(x_1) e^{-i\delta\phi_{A1}} g_{nA}(x_1) e^{i\delta\phi_{A1}} g_{nA}^*(x_2) e^{-i\delta\phi_{A2}} g_{mA}(x_2) e^{i\delta\phi_{A2}} \\ &+ g_{mB}^*(x_1) e^{-i\delta\phi_{B1}} g_{nB}(x_1) e^{i\delta\phi_{B1}} g_{nB}^*(x_2) e^{-i\delta\phi_{B2}} g_{mB}(x_2) e^{i\delta\phi_{B2}}] \\ &= \frac{1}{2} I_0^2. \end{aligned} \quad (45)$$

Likewise, the pair of terms that are constant when doing a spatial scan but dependent on the angular diameter of the source are also overlapped when propagating from the slits to the detectors,

$$\begin{aligned} &\langle \Delta I(x_1)_{AA} \Delta I(x_2)_{BB} \rangle + \langle \Delta I(x_1)_{BB} \Delta I(x_2)_{AA} \rangle \\ &= \frac{I_0}{2\Delta\theta_s} \int_{-\Delta\theta_s/2}^{\Delta\theta_s/2} d\theta_m \frac{I_0}{2\Delta\theta_s} \int_{-\Delta\theta_s/2}^{\Delta\theta_s/2} d\theta_n \frac{1}{\Delta\phi} \int_{-\Delta\phi/2}^{\Delta\phi/2} d\phi_1 \frac{1}{\Delta\phi} \int_{-\Delta\phi/2}^{\Delta\phi/2} d\phi_2 \\ &\times [g_{mA}^*(x_1) e^{-i\delta\phi_{A1}} g_{nA}(x_1) e^{i\delta\phi_{A1}} g_{nB}^*(x_2) e^{-i\delta\phi_{B2}} g_{mB}(x_2) e^{i\delta\phi_{B2}} \\ &+ g_{mB}^*(x_1) e^{-i\delta\phi_{B1}} g_{nB}(x_1) e^{i\delta\phi_{B1}} g_{nA}^*(x_2) e^{-i\delta\phi_{A2}} g_{mA}(x_2) e^{i\delta\phi_{A2}}] \\ &= \frac{1}{2} I_0^2 \text{sinc}^2 \frac{\pi d \Delta\theta_s}{\lambda}. \end{aligned} \quad (46)$$

The terms that mimic the measurement of intensity measured at D_1 see the affect of turbulence,

$$\begin{aligned}
& \langle \Delta I(x_1)_{AB} \Delta I(x_2)_{AA} \rangle + \langle \Delta I(x_1)_{BA} \Delta I(x_2)_{BB} \rangle + \langle \Delta I(x_1)_{AB} \Delta I(x_2)_{BB} \rangle + \langle \Delta I(x_1)_{BA} \Delta I(x_2)_{AA} \rangle \\
&= \frac{I_0}{2\Delta\theta_s} \int_{-\Delta\theta_s/2}^{\Delta\theta_s/2} d\theta_m \frac{I_0}{2\Delta\theta_s} \int_{-\Delta\theta_s/2}^{\Delta\theta_s/2} d\theta_n \frac{1}{\Delta\phi} \int_{-\Delta\phi/2}^{\Delta\phi/2} d\phi_1 \frac{1}{\Delta\phi} \int_{-\Delta\phi/2}^{\Delta\phi/2} d\phi_2 \\
&\times [g_{mA}^*(x_1) e^{-i\delta\phi_{A1}} g_{nB}(x_1) e^{i\delta\phi_{B1}} g_{nA}^*(x_2) e^{-i\delta\phi_{A2}} g_{mA}(x_2) e^{i\delta\phi_{A2}} \\
&+ g_{mB}^*(x_1) e^{-i\delta\phi_{B1}} g_{nA}(x_1) e^{i\delta\phi_{A1}} g_{nB}^*(x_2) e^{-i\delta\phi_{B2}} g_{mB}(x_2) e^{i\delta\phi_{B2}} \\
&+ g_{mA}^*(x_1) e^{-i\delta\phi_{A1}} g_{nB}(x_1) e^{i\delta\phi_{B1}} g_{nA}^*(x_2) e^{-i\delta\phi_{B2}} g_{mB}(x_2) e^{i\delta\phi_{B2}} \\
&+ g_{mB}^*(x_1) e^{-i\delta\phi_{B1}} g_{nA}(x_1) e^{i\delta\phi_{A1}} g_{nA}^*(x_2) e^{-i\delta\phi_{A2}} g_{mA}(x_2) e^{i\delta\phi_{A2}}] \\
&= I_0^2 \text{sinc} \Delta\phi \text{sinc} \frac{\pi d \Delta\theta_s}{\lambda} \cos \frac{2\pi d}{\lambda z} x_1,
\end{aligned} \tag{47}$$

And likewise with the terms that mimic the measurement of intensity measured at D_2 ,

$$\begin{aligned}
& \langle \Delta I(x_1)_{AA} \Delta I(x_2)_{AB} \rangle + \langle \Delta I(x_1)_{BB} \Delta I(x_2)_{BA} \rangle + \langle \Delta I(x_1)_{AA} \Delta I(x_2)_{BA} \rangle + \langle \Delta I(x_1)_{BB} \Delta I(x_2)_{AB} \rangle \\
&= \frac{I_0}{2\Delta\theta_s} \int_{-\Delta\theta_s/2}^{\Delta\theta_s/2} d\theta_m \frac{I_0}{2\Delta\theta_s} \int_{-\Delta\theta_s/2}^{\Delta\theta_s/2} d\theta_n \frac{1}{\Delta\phi} \int_{-\Delta\phi/2}^{\Delta\phi/2} d\phi_1 \frac{1}{\Delta\phi} \int_{-\Delta\phi/2}^{\Delta\phi/2} d\phi_2 \\
&\times [g_{mA}^*(x_1) e^{-i\delta\phi_{A1}} g_{nA}(x_1) e^{i\delta\phi_{A1}} g_{nA}^*(x_2) e^{-i\delta\phi_{A2}} g_{mB}(x_2) e^{i\delta\phi_{B2}} \\
&+ g_{mB}^*(x_1) e^{-i\delta\phi_{B1}} g_{nB}(x_1) e^{i\delta\phi_{B1}} g_{nB}^*(x_2) e^{-i\delta\phi_{B2}} g_{mA}(x_2) e^{i\delta\phi_{A2}} \\
&+ g_{mA}^*(x_1) e^{-i\delta\phi_{A1}} g_{nA}(x_1) e^{i\delta\phi_{A1}} g_{nB}^*(x_2) e^{-i\delta\phi_{B2}} g_{mA}(x_2) e^{i\delta\phi_{A2}} \\
&+ g_{mB}^*(x_1) e^{-i\delta\phi_{B1}} g_{nB}(x_1) e^{i\delta\phi_{B1}} g_{nA}^*(x_2) e^{-i\delta\phi_{A2}} g_{mB}(x_2) e^{i\delta\phi_{B2}}] \\
&= I_0^2 \text{sinc} \Delta\phi \text{sinc} \frac{\pi d \Delta\theta_s}{\lambda} \cos \frac{2\pi d}{\lambda z} x_2.
\end{aligned} \tag{48}$$

The following term is the term of most importance in the turbulence-free double-slit interferometer because, while not always insensitive to turbulence, when scanning such that $x_1 \approx x_2$, the potential paths “overlap.” Because of this we see the random phases introduced by turbulence cancel, i.e. $\delta\phi_{A1} \approx \delta\phi_{A2}$ and $\delta\phi_{B1} \approx \delta\phi_{B2}$, resulting in turbulence-free interference,

$$\begin{aligned}
& \langle \Delta I(x_1)_{AB} \Delta I(x_2)_{BA} \rangle + \langle \Delta I(x_1)_{BA} \Delta I(x_2)_{AB} \rangle \\
&= \frac{I_0}{2\Delta\theta_s} \int_{-\Delta\theta_s/2}^{\Delta\theta_s/2} d\theta_m \frac{I_0}{2\Delta\theta_s} \int_{-\Delta\theta_s/2}^{\Delta\theta_s/2} d\theta_n \frac{1}{\Delta\phi} \int_{-\Delta\phi/2}^{\Delta\phi/2} d\phi_1 \frac{1}{\Delta\phi} \int_{-\Delta\phi/2}^{\Delta\phi/2} d\phi_2 \\
&\times [g_{mA}^*(x_1) e^{-i\delta\phi_{A1}} g_{nB}(x_1) e^{i\delta\phi_{B1}} g_{nB}^*(x_2) e^{-i\delta\phi_{B2}} g_{mA}(x_2) e^{i\delta\phi_{A2}} \\
&+ g_{mB}^*(x_1) e^{-i\delta\phi_{B1}} g_{nA}(x_1) e^{i\delta\phi_{A1}} g_{nA}^*(x_2) e^{-i\delta\phi_{A2}} g_{mB}(x_2) e^{i\delta\phi_{B2}}] \\
&= \frac{1}{2} I_0^2 \cos \frac{2\pi d}{\lambda z} (x_1 - x_2).
\end{aligned} \tag{49}$$

Unlike the previous terms, here the overlap does not cause the cancellation of the random phases, and is actually twice as sensitive to the turbulence present, resulting in a sinc-squared term,

$$\begin{aligned}
& \langle \Delta I(x_1)_{AB} \Delta I(x_2)_{AB} \rangle + \langle \Delta I(x_1)_{BA} \Delta I(x_2)_{BA} \rangle \\
&= \frac{I_0}{2\Delta\theta_s} \int_{-\Delta\theta_s/2}^{\Delta\theta_s/2} d\theta_m \frac{I_0}{2\Delta\theta_s} \int_{-\Delta\theta_s/2}^{\Delta\theta_s/2} d\theta_n \frac{1}{\Delta\phi} \int_{-\Delta\phi/2}^{\Delta\phi/2} d\phi_1 \frac{1}{\Delta\phi} \int_{-\Delta\phi/2}^{\Delta\phi/2} d\phi_2 \\
&\times [g_{mA}^*(x_1) e^{-i\delta\phi_{A1}} g_{nB}(x_1) e^{i\delta\phi_{B1}} g_{nA}^*(x_2) e^{-i\delta\phi_{A2}} g_{mB}(x_2) e^{i\delta\phi_{B2}} \\
&+ g_{mB}^*(x_1) e^{-i\delta\phi_{B1}} g_{nA}(x_1) e^{i\delta\phi_{A1}} g_{nB}^*(x_2) e^{-i\delta\phi_{B2}} g_{mA}(x_2) e^{i\delta\phi_{A2}}] \\
&= \frac{1}{2} I_0^2 \text{sinc}^2 \Delta\phi \text{sinc}^2 \frac{\pi d \Delta\theta_s}{\lambda} \cos \frac{2\pi d}{\lambda z} (x_1 + x_2).
\end{aligned} \tag{50}$$

Combining all of these we get,

$$\begin{aligned} \langle \Delta I(x_1) \Delta I(x_2) \rangle = & \frac{1}{2} I_0^2 \left[1 + \operatorname{sinc}^2 \frac{\pi d \Delta \theta_s}{\lambda} + 2 \operatorname{sinc} \Delta \phi \operatorname{sinc} \frac{\pi d \Delta \theta_s}{\lambda} \cos \frac{2\pi d}{\lambda z} x_1 \right. \\ & + 2 \operatorname{sinc} \Delta \phi \operatorname{sinc} \frac{\pi d \Delta \theta_s}{\lambda} \cos \frac{2\pi d}{\lambda z} x_2 + \cos \frac{2\pi d}{\lambda z} (x_1 - x_2) \\ & \left. + \operatorname{sinc}^2 \Delta \phi \operatorname{sinc}^2 \frac{\pi d \Delta \theta_s}{\lambda} \cos \frac{2\pi d}{\lambda z} (x_1 + x_2) \right], \end{aligned} \quad (51)$$

In the case of strong turbulence, the terms with sinc functions attached will go to zero, resulting in Eq. (32).

Funding

Los Alamos National Laboratory.

Acknowledgments

The authors thank Jane Sprigg and Tao Peng for helpful discussions.

Disclosures

The authors declare no conflicts of interest related to this article.

References

1. E. Hecht, *Optics* (Addison Wesley, 2002).
2. A. R. Thompson, J. M. Moran, and G. W. Swenson Jr, *Interferometry and Synthesis in Radio Astronomy* (John Wiley & Sons, 2001).
3. P. R. Saulson, *Fundamentals of Interferometric Gravitational Wave Detectors* (World Scientific, 1994).
4. D. C. Williams, *Optical Methods in Engineering Metrology* (Chapman and Hall, 1993).
5. D. D. Nolte, *Optical Interferometry for Biology and Medicine* (Springer, 2011).
6. M. E. Brezinski, *Optical Coherence Tomography: Principles and Applications* (Academic, 2006).
7. Z. Y. Ou and L. Mandel, "Measurement of subpicosecond time intervals between two photons by interference," *Phys. Rev. Lett.* **59**(18), 2044–2046 (1987).
8. Y. H. Shih and C. O. Alley, "New type of Einstein-Podolsky-Rosen-Bohm experiment using pairs of light quanta produced by optical parametric down conversion," *Phys. Rev. Lett.* **61**(26), 2921–2924 (1988).
9. J. D. Franson, "Bell inequality for position and time," *Phys. Rev. Lett.* **62**(19), 2205–2208 (1989).
10. R. Hanbury Brown and R. Q. Twiss, "Correlation between photons in two coherent beams of light," *Nature* **177**(4497), 27–29 (1956).
11. R. Hanbury Brown and R. Q. Twiss, "A test of a new type of stellar interferometer on Sirius," *Nature* **178**(4541), 1046–1048 (1956).
12. G. Scarcelli, A. Valencia, and Y. H. Shih, "Two-photon interference with thermal light," *EPL* **68**(5), 618–624 (2004).
13. Y. S. Ihn, Y. Kim, V. Tamma, and Y. H. Kim, "Second-order temporal interference with thermal light: Interference beyond the coherence time," *Phys. Rev. Lett.* **119**(26), 263603 (2017).
14. V. I. Tatarski, *Wave Propagation in a Turbulent Medium*, Translated by R. A. Silverman, (Mcgraw-Hill, 1961).
15. F. Roddier, "The effects of atmospheric turbulence in optical astronomy," *Prog. Opt.* **19**, 281–376 (1981).
16. The LIGO Scientific Collaboration and Virgo Collaboration, "Observation of gravitational waves from a binary black hole merger," *Phys. Rev. Lett.* **116**(6), 061102 (2016).
17. T. A. Smith and Y. H. Shih, "Turbulence-free double-slit interferometer," *Phys. Rev. Lett.* **120**(6), 063606 (2018).
18. T. Young, *A Course of Lectures on Natural Philosophy and the Mechanical Arts*, (Printed for J. Johnson by W. Savage, 1807).
19. Y. H. Shih, *An Introduction to Quantum Optics: Photon and Biphoton Physics* (CRC press, Taylor & Francis, 1st edition, 2011).
20. G. Scarcelli, V. Berardi, and Y. H. Shih, "Can two-photon correlation of chaotic light be considered as correlation of intensity fluctuations?" *Phys. Rev. Lett.* **96**(6), 063602 (2006).
21. A. Einstein, "Concerning an heuristic point of view toward the emission and transformation of light," *Ann. Phys.* **322**(6), 132–148 (1905).
22. R. J. Glauber, "The quantum theory of optical coherence," *Phys. Rev.* **130**(6), 2529–2539 (1963).
23. M. O. Scully and M. S. Zubairy, *Quantum Optics*, (Cambridge University, 1997).
24. W. Martienssen and E. Spiller, "Coherence and fluctuations in light beams," *Am. J. Phys.* **32**(12), 919–926 (1964).
25. H. Chen, T. Peng, and Y. H. Shih, "100% correlation of chaotic thermal light," *Phys. Rev. A* **88**(2), 023808 (2013).